Configurational correlations in the coverage dependent adsorption energies of oxygen atoms on late transition metal fcc(111) surfaces

ARTICLE *in* THE JOURNAL OF CHEMICAL PHYSICS · MARCH 2011

Impact Factor: 2.95 · DOI: 10.1063/1.3561287 · Source: PubMed

3 AUTHORS, INCLUDING:

John R. Kitchin
Carnegie Mellon University
94 PUBLICATIONS **3,668** CITATIONS

Configurational correlations in the coverage dependent adsorption energies of oxygen atoms on late transition metal fcc(111) surfaces

Spencer D. Miller, Nilay İnoğlu, and John R. Kitchin[a)]
Department of Chemical Engineering, Carnegie Mellon University, Pittsburgh, Pennsylvania 15213, USA

(Received 20 December 2010; accepted 10 February 2011; published online 14 March 2011)

The coverage dependence of oxygen adsorption energies on the fcc(111) surfaces of seven different transition metals (Rh, Ir, Pd, Pt, Cu, Au, and Ag) is demonstrated through density functional theory calculations on 20 configurations ranging from one to five adsorption sites and coverages up to 1 ML. Atom projected densities of states are used to demonstrate that the *d*-band mediated adsorption mechanism is responsible for the coverage dependence of the adsorption energies. This common bonding mechanism results in a linear correlation that relates the adsorption energies of each adsorbate configuration across different metal surfaces to each other. The slope of this correlation is shown to be related to the characteristics of the valence *d*-orbitals and band structure of the surface metal atoms. Additionally, it is shown that geometric similarity of the configurations is essential to observe the configurational correlations. © *2011 American Institute of Physics*. [doi:10.1063/1.3561287]

I. INTRODUCTION

Transition metal surfaces commonly play a role as catalysts in industrial processes, often with oxygen either directly involved or present in the environment. The interaction of oxygen with these surfaces to form chemisorbed states can occur either as part of the catalyzed reaction chain, or as the first step toward the oxidation of the surface which can serve either to deactivate its catalytic properties or in some cases to enhance them.[1] The importance of these oxygen transition metal surface systems has provided a rich field for study both experimentally and computationally over the past half century.

Experimental studies typically occur in ultrahigh vacuum conditions and utilize a selection of spectroscopic (e.g., XPS, AES, LEED, and others) or thermal desorption [temperature programmed desorption (TPD)] techniques to characterize the adsorbed species present on metal surfaces after exposure to oxygen (either in the form of molecular oxygen or oxygen precursors such as O_3 and NO_2). The low Miller index surfaces are frequently studied because they generally compose the majority of facets on particles due to their low surface energies. For the (111) surface in particular, a large number of studies have been conducted on a wide range of late transition metal surfaces including Rh,[2–6] Ir,[7–12] Pd,[13–15] Pt,[16–19] Cu,[20–31] Ag,[32–36] and Au.[37–47] Coverage dependence in the adsorption behavior of oxygen is a common theme through much of the experimental work, including coverage dependent desorption barriers and the formation of surface and bulk oxide structures.

While experimental studies provide direct measurements of some adsorption properties of the adsorbate–metal system, the data collected can be difficult to interpret; this is especially true when there is uncertainty in the state of the surface itself. One example of the difficulty posed by this uncertainty can be found in TPD studies[3,5,6,10,12–15,32,34,39,42] which seek to calculate the energy barrier for the desorption of chemisorbed oxygen. In many of these studies the surface is exposed to oxygen well past the point of surface oxidation.[3,32,39] It is difficult to determine when exactly oxide formation begins to take place, and the resulting TPD spectra, which include both chemisorbed states and oxide structures at higher coverages can be difficult to interpret in traditional Redhead terms. It is difficult to determine the saturation coverage of chemisorbed atoms, especially when surface oxidation begins. As an example of this difficulty, in one particular study of oxygen desorption from Au(111),[39] the characteristic shape of the desorption peaks resulting from the oxide structures appeared to take first-order form, which leads to the interpretation of what is most likely a second-order associative desorption process with a first-order rate law model.

Computational studies provide the advantage of full control over the adsorption configurations being studied, allowing chemisorption to be studied in detail with direct specification of the adsorbate coverage, configuration, and chemisorbed state. Density functional theory (DFT) calculations allow the energies of these desired configurations to be calculated, and while the energies are understood to deviate from the experimentally known values due to approximations in the DFT framework, the energy trends tend to be captured accurately.[48–51] Many DFT studies have been conducted for oxygen adsorption on the same set of transition metals discussed above: Rh,[52] Ir,[53] Pd,[54,55] Pt,[49,56–58]Cu,[59] Ag,[36,60,61]and Au.[49,62]

An electronic structure mechanism, mediated through the *d*-bands of the surface metal atoms, has been identified as a major factor in the coverage dependence of the adsorption on transition metal surfaces.[63,64] This *d*-band model was found applicable to the coverage dependent adsorption energies of the atomic adsorbates C, N, and O on Pd(111) (Ref. 55) and for oxygen adsorption on Au and Pt(111).[49] It was found that due to this shared underlying adsorption

a)Electronic mail: jkitchin@andrew.cmu.edu.

mechanism that the adsorption energies of these adsorbates on the two metal surfaces in the same configurations were linearly correlated; a relationship deemed the "configurational correlation" because it correlates the adsorption energies of the same configuration between two metal surfaces. This relationship was not a result of a specific relationship between Au and Pt, but instead was the result of the common underlying bonding mechanism thought to apply to oxygen adsorption on all late transition metals. Although the adsorption of oxygen on these metals has been a common field of study as discussed above, there was still a need for a set of consistent (e.g., computed with the same computational parameters) calculations on a wide set of late transition metal surfaces to demonstrate the generality of the configurational correlation and the universality of the underlying bonding mechanism on these surfaces.

In this work we present such a set of DFT calculations which we use to study both the *d*-band mediated adsorption mechanism that is common to oxygen adsorption on late transition metals, and the configurational correlation that exists because of it. Specifically, DFT calculations were performed for oxygen adsorption on the fcc(111) surfaces of the following late transition metals: Rh, Ir, Pd, Pt, Cu, Ag, and Au. From these DFT calculations both the coverage dependent adsorption energies and the *d*-band structures were extracted. We demonstrate the *d*-band mechanism, which relates changes in adsorption energy to increased coverage through electronic structure modifications of the metal surface *d*-bands, and show that it effectively explains the coverage dependence of the oxygen adsorption energies for these surfaces. We then demonstrate the generality of the configurational correlation for the late transition metals by correlating their adsorption energies against those of Pd(111). We also observe that geometric dissimilarity can lead to poor correlation. Finally, we relate the slopes of the configurational correlation to the characteristics of the surface metal *d*-orbitals and band structure.

II. METHODS

First principles *ab initio* DFT calculations were performed using DACAPO,[65] with the Perdew–Wang 91 [generalized gradient approximation (GGA)] (Ref. 66) exchange-correlation functional, and ultrasoft Vanderbilt pseudopotentials.[67] Four layer fcc(111) slabs were used for each of the seven metals: Rh, Ir, Pd, Pt, Cu, Ag, and Au, with the bottom two layers fixed in bulk positions. Twenty different nonzero coverage oxygen adsorption configurations were considered ranging in size from one to five adsorption sites.[55] A ($12 \times 12 \times 1$) *k*-point Monkhorst–Pack grid was used for the p(1×1) unit cell, with larger cells using a commensurate *k*-point grid of the same density. Plane wave cutoff energies of 350 eV were utilized throughout. Lattice constants were determined computationally using the Murnaghan equation of state,[68] and are as follows: 3.82 Å for Rh, 3.85 Å for Ir, 3.92 Å for Pd, 4.02 Å for Pt, 3.68 Å for Cu, 4.14 Å for Ag, and 4.19 Å for Au. Oxygen is known to prefer the fcc hollow site on all of the surfaces studied in this work,[49,52–59,61,62] and only fcc hollow adsorption sites are considered for all configurations used.

Adsorption energies were calculated on a per adsorbate basis with reference to atomic oxygen as shown in the following equation:

$$\Delta H_{\text{ads}} = \frac{E_{\text{M-O}} - E_{\text{M}} - N_{\text{O}} \cdot E_{\text{O}}}{N_{\text{O}}}, \tag{1}$$

where ΔH_{ads} is the adsorption energy, $E_{\text{M-O}}$ is the total energy of the metal slab with adsorbed oxygen atoms, E_{M} is the energy of the clean metal surface, N_{O} is the number of oxygen atoms adsorbed on the surface, and E_{O} is the energy of a single oxygen atom in vacuum. The atomic reference state was chosen as a matter of convenience, and has no ramification on the conclusions drawn in this work; a molecular reference state simply shifts all adsorption energies by a constant amount.

III. RESULTS AND DISCUSSION

The results of the DFT calculations described above were utilized to calculate adsorption energies normalized by the number of oxygen adsorbates in the configuration, as shown in Eq. (1). These adsorption energies vary consistently with oxygen coverage: increasing (corresponding to a weakening of the adsorption bond) with increasing coverage, shown in Fig. 1. This roughly linear trend is consistent across all seven metal surfaces and is consistent with previous coverage dependent oxygen adsorption energy studies on some of the considered surfaces (Pd, Pt, Au, and Ag).[49,55–57,61,62] The configurations considered in this study include only chemisorbed species of oxygen. It is known experimentally that oxides, including surface oxide structures, form on all of these metal surfaces at sufficiently high oxygen chemical potentials and

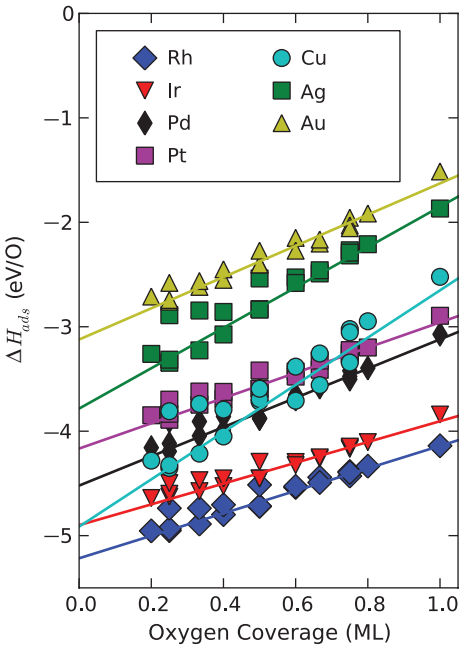

FIG. 1. Adsorption energy (eV/O) vs coverage (ML) for oxygen adsorption on the Rh, Ir, Pd, Pt, Cu, Ag, and Au(111) surfaces for 20 configurations.

coverages. In the case of Pt(111) surface oxides have been observed at coverages of less than 0.5 ML,[19] while in the noble metals such as Ag and Au(111) surface oxides form so readily that it is difficult to observe the chemisorbed state of oxygen on these surfaces before the onset of oxide formation.[32,39] Thus, the observations derived from these calculations apply directly only to a narrow window of adsorption where chemisorption is the dominant mechanism or to cases in which surface oxide formation is kinetically inhibited. While experimentally this may only govern a small feasible range of oxygen coverages, it retains certain advantages in terms of ease of computational study. The trends and characteristics of these chemisorption processes can help reveal general adsorption behavior, which may in future work aid in developing an understanding of more complicated adsorption regimes. Therefore, even though many of the specific configurations studied in this work may not be directly relevant to experimentally observed states, the underlying adsorption mechanisms they reveal aid our general understanding of adsorption behavior.

The coverage dependence of the adsorption energies can be understood in terms of the *d*-band mediated model as previously demonstrated for oxygen adsorption on the Au and Pt(111) surfaces[49] and for C, N, O, on Pd(111).[55] This model directly relates changes in the *d*-bands of the surface metal atoms caused by the presence of adsorbate atoms on the surface to the observed weakening of adsorption energies. As the oxygen coverage (θ) increases, the overlap between the *s–p* orbitals of the oxygen adsorbates and the valence *d*-orbitals of the surface metal atoms increases. This increased overlap results in a broadening of the surface metal atom *d*-bands. The *d*-band density of states of the surface metal atoms and the *s–p* density of states of the adsorbate oxygen atoms have been estimated by calculating the atom projected density of states for the DFT calculations described above, using an infinite cutoff radius. The infinite cutoff, while overestimating the filling of the *d*-bands in some cases, provides improved accuracy for larger metal atoms, such as Ir, which may not have their full electron shell within a smaller cutoff radius. Figure 2 shows the characteristic behavior of the *d*-band for the Pd(111) surface where the *d*-band density of states shown is averaged over all surface metal atoms. As coverage increases, the width of the *d*-band is also found to increase, a result of increased overlap between the electron orbitals of the adsorbates and the surface metal atoms. Additionally, as the *d*-band broadens, the *d*-band center (as indicated by the solid red vertical line) is observed shifting to lower energies away from the Fermi level. The number of *d* electrons remains approximately constant with changing coverage, although a slight trend toward a decrease in the number of electrons is observed; this would be consistent with a small amount of charge transfer to the adsorbed oxygen atoms due to the partial oxidation of the surface by the adsorbates.

This relationship between the width and the center of the *d*-band can be understood through the rectangular band model. If the shape of the *d*-band is considered rectangular, provided that the filling of the *d*-band is constant, then geometrically the center of the *d*-band will shift to lower energies as the width of the *d*-band increases. With the center of the

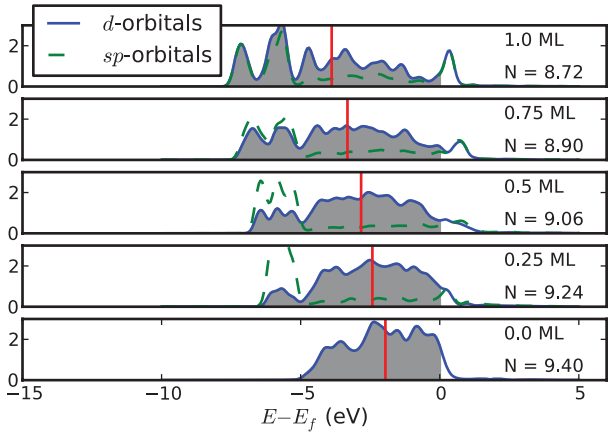

FIG. 2. Atom projected density of states for five configurations of O on Pd(111) with coverages varying from 0 ML (bottom) to 1.0 ML (top). The density of states of the surface metal *d*-bands, averaged over all surface metal atoms, are shown with grey filling up to the Fermi level. The density of states of the *s-p* orbitals of the adsorbates, averaged over each adsorbate, is shown as a dashed line with no filling. The *d*-band center, defined as the first moment of the *d*-band, is shown as a vertical line for each configuration. The number of electrons in the valence *d*-band (N), calculated by integration of the density of states up to the Fermi level, is shown for each configuration.

d-band defined as the first moment of the projected *d*-band about the Fermi level, the rectangular band model predicts a linear relationship exists between the center and the width, with a slope dependent on the *d*-band filling. A linear relationship between the *d*-band width and *d*-band center exists whether the width is defined as the energy difference between the highest and lowest states of the band, or as the square root of the second moment of the *d*-band.[69] For the remainder of this work the *d*-band width will be defined as the square root of the second moment of the *d*-band with respect to the Fermi level, and the *d*-band center as the first moment of the *d*-band with respect to the Fermi level. Figure 3 shows that the centers of the *d*-band vary linearly with changes in the *d*-band width for all of the metal surfaces in this work. Therefore, as increasing adsorbate coverages cause a broadening of the *d*-band, the *d*-band center experiences a corresponding shift to lower energies.

The Hammer–Nørskov model[70] relates a decrease in the energy of the *d*-band center to the decreased stability of an adsorption bond—an increase in the adsorption energy. This change in adsorption energy is related to the occupation of antibonding orbitals which exist near the Fermi level: as the *d*-band center shifts to lower energies, a greater number of these antibonding orbitals become occupied, resulting in the weakening of the adsorption bond. In Fig. 4 the *d*-band center is shown versus the adsorption energy for the Rh, Ir, Pd, and Pt(111) metal surfaces. In each case, the adsorption energy versus *d*-band center relationship is found to follow a roughly linear trend. This is consistent with the Hammer–Nørskov model. Therefore, as increased adsorbate coverage on the surface widens the *d*-band due to the increased overlap of electron orbitals, a corresponding shift in the *d*-band center to lower energies is observed due to the rectangular band model, which is then related to an increase in the adsorption energies according to the Hammer–Nørskov model. This overall

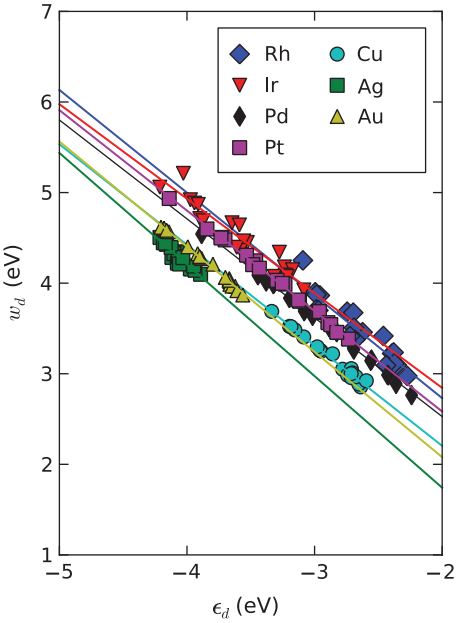

FIG. 3. The *d*-band width vs the *d*-band center for O on Rh, Ir, Pd, Pt, Cu, Ag, and Au(111) demonstrating the linear dependence expected from the rectangular band model.

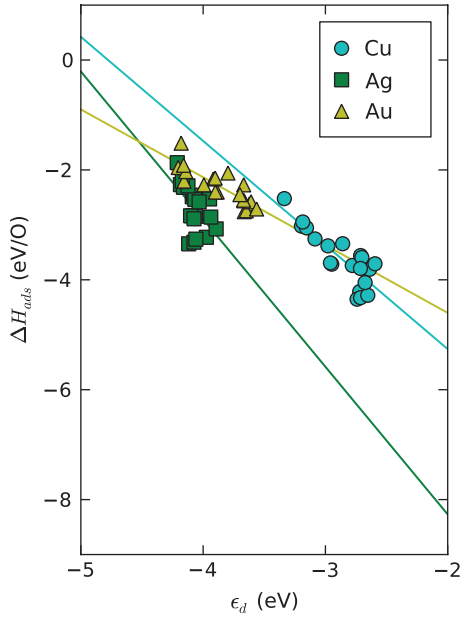

FIG. 5. Adsorption energy vs the *d*-band center for O on Cu, Ag, and Au(111) demonstrating that despite a fully filled valence *d*-band the linear dependence expected from the Hammer–Nørskov model is still present. The coefficient of determination (R^2) values for the linear fits are 0.71 for Cu, 0.71 for Au, and 0.30 for Ag.

relationship is consistent with the trends in adsorption energies as shown in Fig. 1.

The noble metals, such as Ag, Au, and Cu, possess fully filled valence *d*-shells. The interaction between the renormalized *s–p* orbitals of the oxygen adsorbates and the *d*-band of the surface metal atoms includes an increased contribution from Pauli repulsion that works in the opposite direction of the antibonding orbital occupation mechanism. As the *d*-band center shifts to lower energies the Pauli repulsion weakens. Xin and Linic showed that in cases where Pauli repulsion plays a dominant role, such as the interaction between a OH adsorbate with a nearly filled *s–p* orbital and d^9 and d^{10} metal surfaces, the increased contribution of this repulsion completely reverses the trend expected by the Hammer–Nørskov model.[71] Although the atomic oxygen adsorbate is not a closed shell adsorbate for which the *d*-band model was found to be insufficient, the increased role of Pauli repulsion could render the *d*-band center alone insufficient to fully describe the coverage dependence of the adsorption energies; however, plotting the adsorption energies versus the *d*-band centers for the Ag, Au, and Cu surfaces in Fig. 5 we find that, in general, the systems behave as expected under the *d*-band model, although Ag shows the weakest correlation. This suggests that although the filled valence *d*-band slightly alters the physics of adsorption in the case of the noble metals such as Ag, the *d*-band mediated mechanism is sufficient to capture the majority of the coverage dependent adsorption energy trends even of these noble metal systems.

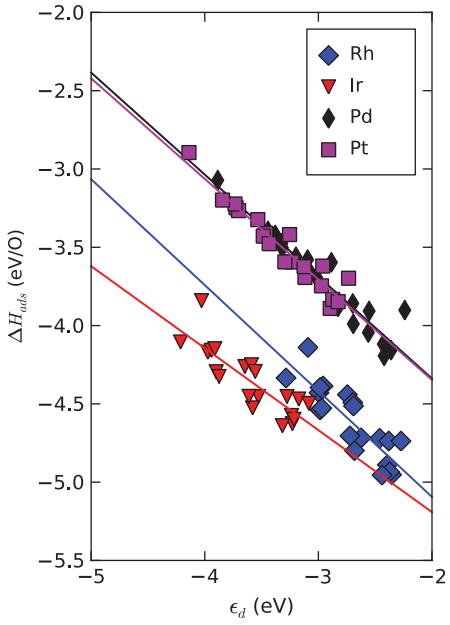

FIG. 4. Adsorption energy vs the *d*-band center for O on Rh, Ir, Pd, and Pt(111) demonstrating the linear dependence expected from the Hammer–Nørskov model.

Previously, the coverage dependent adsorption energies of oxygen adsorption on Au and Pt(111) were shown to be linearly related to one another.[49] This correlation has been called "the configurational correlation" as it relates the adsorption energy of a given configuration across different metal surfaces to the same configuration on a reference metal. The existence of this correlation was proposed to be due to the *d*-band mediated coverage dependent adsorption mechanism common to the late transition metals. Figure 6 shows the adsorption energies for each nonzero coverage configurations of O on Rh, Ir, Pt, Cu, Ag, and Au(111) plotted against the energy of the same configuration on the Pd(111) surface. The linear relationship previously observed to exist between the

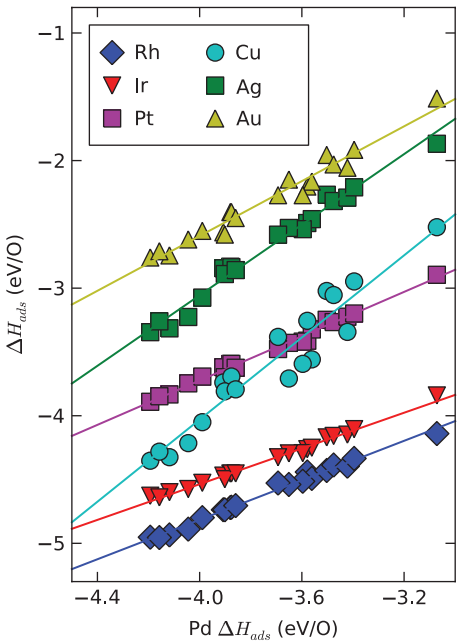

FIG. 6. The configurational correlation: the adsorption energy of each configuration of O on Rh, Ir, Pt, Cu, Ag, and Au(111) plotted against the energy of the same configuration on Pd(111), with best fit lines shown for each metal.

Au and Pt(111) surfaces is also found between the adsorption energies on all of these metals, with best fit lines based on a least squares fit plotted for each surface. The average absolute error from this fit was less than 22 meV/O for the Ir, Pt, and Rh surfaces, which is similar to the 20 meV/O convergence errors in the DFT calculations themselves. This error was greater on the noble metal surfaces: with average errors of 55 meV/O on Ag and Au, and 120 meV/O on Cu.

Inspection of the relaxed Cu configurations revealed significant displacements of the Cu atoms from their initial positions in the presence of oxygen, especially in the z-axis of the surfaces, with some surface Cu atoms lifting out of the surface. These reconstructions cause a significant amount of geometric dissimilarity between the Cu configurations and the reference Pd configurations they are being correlated against, an example of which is shown in Fig. 7. Such reconstructions fundamentally alter the bonding mechanism and electronic structure behavior that is being correlated by changing the positions of the atoms and the resulting overlap between the electronic orbitals. The configurational correlation is, in essence, a correlation between the energies of configurations rather than coverages, and relies on the configurations being compared to be geometrically similar.

To confirm that this geometric dissimilarity was the origin of the poor correlation of the noble metal configurations, a new set of DFT calculations was performed for the Cu, Ag, and Au configurations where the atoms were fixed in the corresponding relaxed configuration on Pd, scaled by the ratio of lattice constants. The correlation between the adsorption energies on the scaled coordinates with the corresponding Pd adsorption energies showed significant improvement with the average error for Au improving from 55 to 24 meV/O, for Ag slightly improving from 55 to 46 meV/O, and Cu's average error was cut nearly in half to 65 meV/O. The configurational correlation for Cu and Pd for both geometrically similar and dissimilar configurations is shown in Fig. 8, where the improvement in the correlation behavior can be clearly observed.

The slopes of the configurational correlations are of particular interest because they are related to the adsorption characteristics of oxygen on each metal surface. It was empirically found that the slope of the correlation depended both on the characteristic radius (r_d) of the surface metal atom d-orbitals, a value which can be found in the solid state table,[72] and which is related to the size of the metal atom's valence d-orbital with additional dependence on the cube of the d-band filling (f_d). Using the model in Eq. (2), which relates the configuration correlation slopes to ratios of these two valence d-band characteristics, where m is the slope of the configurational correlation, subscript M refers to the metal in question, Pd is the metal being used as the reference, and κ is an empirically determined constant (found to be 0.976 by least squares fitting to the six known slopes), it was possible to explain the trends in the slopes for the configurational

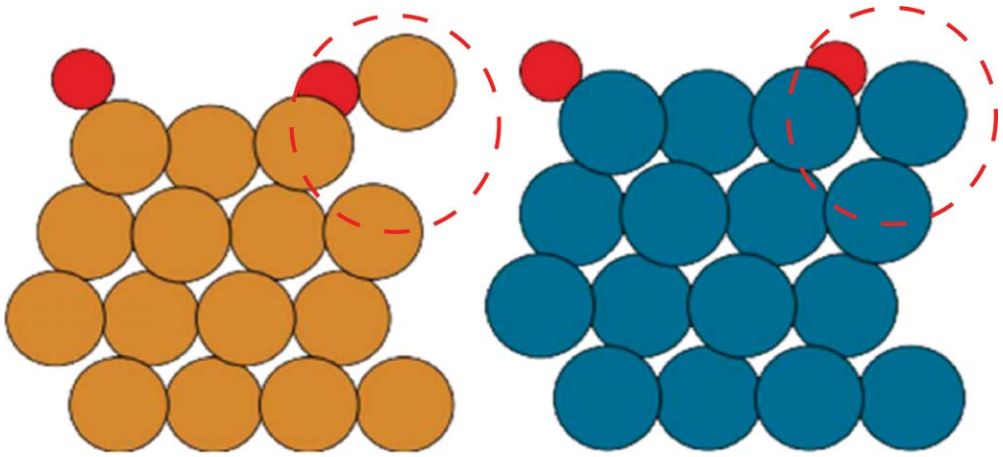

FIG. 7. Example reconstruction: the Cu configuration is shown on the left, and the Pd configuration is shown on the right, with the oxygen adsorbates appearing as the smaller atoms near the surface (at the top of each configuration). One of the Cu surface metal atoms has lifted out of the surface during relaxation resulting in geometrically dissimilar relaxed configurations.

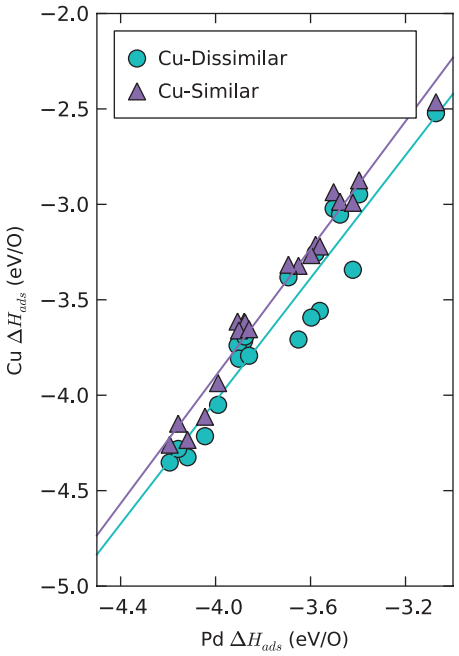

FIG. 8. The configurational correlation for O on Cu(111) vs Pd(111) for both geometrically similar and dissimilar Cu configurations.

correlations as shown in Table I.

$$m = \kappa \left(\frac{r_{d,\mathrm{Pd}}}{r_{d,\mathrm{M}}}\right)\left(\frac{f_{d,\mathrm{M}}}{f_{d,\mathrm{Pd}}}\right)^3. \quad (2)$$

The characteristic radius can be used to relate changes in coverage to changes in the *d*-band width, due to its representation of the size of the valence *d*-orbitals and hence the overlap between orbitals. The *d*-band width is linearly related to the *d*-band center via the rectangular band model, and the *d*-band filling determines the relationship between changes in the *d*-band center and the *d*-band width. The higher the *d*-band filling is, the higher the slope of the configurational correlation. Thought of in other terms: the higher the *d*-band filling is, the greater the change in adsorption energy for a given change in coverage; the more difficult it is to adsorb additional oxygen atoms onto the surface, due to both the decreased favorability of the thermodynamics as well as a related increase in the kinetic barriers associated with noble metals.[73]

TABLE I. Parameters [characteristic radii (r_d) and fractional filling of the valance *d*-band (f)] for use in model for prediction of configurational correlation slope [Eq. (2)] with the predicted slope (m_{model}), the slope calculated from the DFT results (m_{DFT}), and the difference between the slopes ($|\Delta m|$).

Metal	r_d[a]	f	m_{model}	m_{DFT}	$\lvert\Delta m\rvert$
Rh	3.32	0.8	0.87	0.77	0.1
Ir	3.72	0.8	0.62	0.70	0.08
Pd	3.38	0.9	1.00	1.00	...
Pt	3.79	0.9	0.87	0.87	0.00
Cu	2.68	1.0	1.69	1.61	0.08
Ag	3.34	1.0	1.36	1.38	0.02
Au	3.88	1.0	1.17	1.07	0.1

[a]Reference 72.

IV. CONCLUSION

The trends in coverage dependent adsorption energies for oxygen adsorption on the Rh, Ir, Pd, Pt, Cu, Ag, and Au(111) surfaces have been calculated utilizing DFT. They display similar, roughly linear, trends with increasing adsorption energies as coverage increases. The source of this coverage dependence has been discussed in terms of the *d*-band mediated model, which was shown to be a common mechanism general to oxygen adsorption on the late transition metals.

Due to this shared coverage dependent adsorption mechanism, the adsorption energies of these systems are also demonstrated to correlate linearly—provided that the geometries are similar. We have shown that this configurational correlation applies universally to oxygen adsorption on the late transition metals. The slopes of these correlations are found to be related to both the characteristic radius of the metal surface atom *d*-orbitals, and their valence *d*-band filling.

ACKNOWLEDGMENTS

This work was funded by the Department of Energy, Office of Basic Energy Science (Grant No. DOE-BES DEFG0207ER15919).

[1]H. Over, Y. D. Kim, A. P. Seitsonen, S. Wendt, E. Lundgren, M. Schmid, P. Varga, A. Morgante, and G. Ertl, Science **287**, 1474 (2000).
[2]J. T. Yates, P. A. Thiel, and W. H. Weinberg, Surf. Sci. **84**, 427 (1979).
[3]T. W. Root, L. D. Schmidt, and G. B. Fisher, Surf. Sci. **134**, 30 (1983).
[4]C. T. Reimann, M. Elmaazawi, K. Walzl, B. J. Garrison, N. Winograd, and D. M. Deaven, J. Chem. Phys. **90**, 2027 (1989).
[5]K. A. Peterlinz and S. J. Sibener, J. Phys. Chem. **99**, 2817 (1995).
[6]P. A. Thiel, J. T. Yates, and W. H. Weinberg, Surf. Sci. **82**, 22 (1979).
[7]T. S. Marinova and K. L. Kostov, Surf. Sci. **185**, 203 (1987).
[8]D. I. Hagen, B. E. Nieuwenhuys, G. Rovida, and G. A. Somorjai, Surf. Sci. **57**, 632 (1976).
[9]P. A. Zhdan, G. K. Boreskov, and A. I. Boronin, Surf. Sci. **61**, 25 (1976).
[10]V. P. Ivanov, G. K. Boreskov, and V. I. Savchenko, Surf. Sci. **61**, 207 (1976).
[11]H. Conrad, J. Kuppers, F. Nitschke, and A. Plagge, Surf. Sci. **69**, 668 (1977).
[12]J. C. L. Cornish and N. R. Avery, Surf. Sci. **235**, 209 (1990).
[13]H. Conrad, G. Ertl, J. Kuppers, and E. E. Latta, Surf. Sci. **65**, 235 (1977).
[14]H. Conrad, G. Ertl, J. Kuppers, and E. E. Latta, Surf. Sci. **65**, 245 (1977).
[15]G. Zheng and E. I. Altman, Surf. Sci. **462**, 151 (2000).
[16]B. C. Stipe, M. A. Rezaei, and W. Ho, J. Chem. Phys. **107**, 6443 (1997).
[17]J. Wintterlin, R. Schuster, and G. Ertl, Phys. Rev. Lett. **77**, 123 (1996).
[18]D. H. Parker, M. E. Bartram, and B. E. Koel, Surf. Sci. **217**, 489 (1989).
[19]S. P. Devarajan, J. A. Hinojosa, and J. F. Weaver, Surf. Sci. **602**, 3116 (2008).
[20]F. Jensen, F. Besenbacher, E. Laegsgaard, and I. Stensgaard, Surf. Sci. **259**, L774 (1991).
[21]L. H. Dubois, Surf. Sci. **119**, 399 (1982).
[22]H. Niehus, Surf. Sci. **130**, 41 (1983).
[23]J. Haase and H. J. Kuhr, Surf. Sci. **203**, L695 (1988).
[24]G. Ertl, Surf. Sci. **6**, 208 (1967).
[25]G. W. Simmons, D. F. Mitchell, and K. R. Lawless, Surf. Sci. **8**, 130 (1967).
[26]R. W. Judd, P. Hollins, and J. Pritchard, Surf. Sci. **171**, 643 (1986).
[27]F. H. P. M. Habraken, E. P. Kieffer, and G. A. Bootsma, Surf. Sci. **83**, 45 (1979).
[28]F. H. P. M. Habraken, C. M. A. M. Mesters, and G. A. Bootsma, Surf. Sci. **97**, 264 (1980).
[29]R. C. Baetzold, Surf. Sci. **95**, 286 (1980).
[30]L. J. Hanekamp, W. Lisowski, and G. A. Bootsma, Surf. Sci. **118**, 1 (1982).
[31]A. Spitzer and H. Luth, Surf. Sci. **118**, 136 (1982).
[32]C. T. Campbell, Surf. Sci. **157**, 43 (1985).

[33]C. T. Campbell, Surf. Sci. **173**, L641 (1986).
[34]S. R. Bare, K. Griffiths, W. N. Lennard, and H. T. Tang, Surf. Sci. **342**, 185 (1995).
[35]C. I. Carlisle, T. Fujimoto, W. S. Sim, and D. A. King, Surf. Sci. **470**, 15 (2000).
[36]J. Schnadt, J. Knudsen, X. L. Hu, A. Michaelides, R. T. Vang, K. Reuter, Z. S. Li, E. Laegsgaard, M. Scheffler, and F. Besenbacher, Phys. Rev. B **80**, 075424 (2009).
[37]M. A. Chesters and G. A. Somorjai, Surf. Sci. **52**, 21 (1975).
[38]M. E. Schrader, Surf. Sci. **78**, L227 (1978).
[39]N. D. S. Canning, D. Outka, and R. J. Madix, Surf. Sci. **141**, 240 (1984).
[40]P. Legare, L. Hilaire, M. Sotto, and G. Maire, Surf. Sci. **91**, 175 (1980).
[41]J. J. Pireaux, M. Chtaib, J. P. Delrue, P. A. Thiry, M. Liehr, and R. Caudano, Surf. Sci. **141**, 211 (1984).
[42]N. Saliba, D. H. Parker, and B. E. Koel, Surf. Sci. **410**, 270 (1998).
[43]L. Ortega, L. Huang, J. Chevrier, P. Zeppenfeld, J. M. Gay, F. Rieutord, and G. Comsa, Surf. Rev. Lett. **4**, 1315 (1997).
[44]L. Huang, P. Zeppenfeld, J. Chevrier, and G. Comsa, Surf. Sci. **352**, 285 (1996).
[45]L. Huang, J. Chevrier, P. Zeppenfeld, and G. Cosma, Appl. Phys. Lett. **66**, 935 (1995).
[46]J. Chevrier, L. Huang, P. Zeppenfeld, and G. Comsa, Surf. Sci. **355**, 1 (1996).
[47]Y. Uchida, X. Bao, K. Weiss, and R. Schlogl, Surf. Sci. **401**, 469 (1998).
[48]J. R. Kitchin, S. D. Miller, and D. S. Sholl, "Density functional theory studies of alloys in heterogeneous catalysis," in *Specialist Periodical Reports: Chemical Modeling: Applications and Theories* (RSC, Cambridge, 2008).
[49]S. D. Miller and J. R. Kitchin, Surf. Sci. **603**, 794 (2009).
[50]B. Hammer and J. K. Nørskov, Adv. Catal. **45**,71 (2000).
[51]J. Greeley, J. K. Nørskov, and M. Mavrikakis, Annu. Rev. Phys. Chem. **53**, 319 (2002).
[52]M. Mavrikakis, J. Rempel, J. Greeley, L. B. Hansen, and J. K. Norskov, J. Chem. Phys. **117**, 6737 (2002).
[53]Y. Xu and M. Mavrikakis, J. Chem. Phys. **116**, 10846 (2002).
[54]M. Todorova, K. Reuter, and M. Scheffler, J. Phys. Chem. B **108**, 14477 (2004).
[55]J. R. Kitchin, Phys. Rev. B **79**, 205412 (2009).
[56]H. R. Tang, A. Van Der Ven, and B. L. Trout, Phys. Rev. B **70**, 045420 (2004).
[57]R. B. Getman, Y. Xu, and W. F. Schneider, J. Phys. Chem. C **112**, 9559 (2008).
[58]D. C. Ford, Y. Xu, and M. Mavrikakis, Surf. Sci. **587**, 159 (2005).
[59]Y. Xu and M. Mavrikakis, Surf. Sci. **494**, 131 (2001).
[60]A. Michaelides, K. Reuter, and M. Scheffler, J. Vac. Sci. Technol. A **23**, 1487 (2005).
[61]W. X. Li, C. Stampfl, and M. Scheffler, Phys. Rev. B **65**, 075407 (2002).
[62]H. Shi and C. Stampfl, Phys. Rev. B **76**, 075327 (2007).
[63]B. Hammer, Phys. Rev. B **6320**, 205423 (2001).
[64]K. A. Fichthorn and M. Scheffler, "Substrate-mediated interaction on Ag(111) surfaces from first principles," in *Collective Diffusion on Surfaces: Correlation Effects and Adatom Interactions*, edited by M. C. Tringides and Z. Chvoj (Kluwer Academic, Boston, 2001), pp. 225–236.
[65]B. Hammer, L. B. Hansen, and J. K. Nørskov, Phys. Rev. B **59**, 7413 (1999).
[66]J. P. Perdew and Y. Wang, Phys. Rev. B **45**, 13244 (1992).
[67]D. Vanderbilt, Phys. Rev. B **41**, 7892 (1990).
[68]F. D. Murnaghan, Proc. Natl. Acad. Sci. U.S.A. **30**, 244 (1944).
[69]J. R. Kitchin, J. K. Nørskov, M. A. Barteau, and J. G. Chen, J. Chem. Phys. **120**, 10240 (2004).
[70]B. Hammer and J. K. Nørskov, Surf. Sci. **343**, 211 (1995).
[71]H. L. Xin and S. Linic, J. Chem. Phys. **132**, 221101 (2010).
[72]N. Inoglu and J. R. Kitchin, Mol. Simul. **36**(7–8), 633 (2010).
[73]Y. Xu, A. V. Ruban, and M. Mavrikakis, J. Am. Chem. Soc. **126**, 4717 (2004).